VIA MEDICA

Artykuł oryginalny / Original article

Biuletyn Polskiego
Towarzystwa Onkologicznego
NOWOTWORY
2023, tom 8, nr 1, 10–17

ISSN: 2543–5248, e-ISSN: 2543–8077
www.nowotwory.edu.pl

The prototype of EPID-based *in vivo* dose verification for VMAT treatments in patients with prostate cancer

Krzysztof Ślosarek[1], Adam Gądek[1], Marta Reudelsdorf-Ullmann[1], Łukasz Sroka[1], Janusz Winiecki[2, 3]

[1]*Radiotherapy Planning Department, Maria Sklodowska-Curie National Research Institute of Oncology, Gliwice Branch, Gliwice, Poland*
[2]*Medical Physics Department, Oncology Center in Bydgoszcz, Bydgoszcz, Poland*
[3]*Department of Oncology and Brachytherapy, Collegium Medicum in Bydgoszcz, Nicholas Copernicus University in Toruń, Bydgoszcz, Poland*

Introduction. The volumetric modulated arc therapy technique (VMAT) is now widely used in radiotherapy. Verification of the dose delivered to the patient is performed prior to the treatment (pre-treatment mode). However, during the therapeutic session, only the patient's position is verified and monitored. AnEPID's (electronic portal imaging device) matrices can measure the intensity of radiation passing through the patient, but the calculation of the dose distribution from this measurement is limited due to the lack of reliable algorithms and software. Therefore, it seems promising to develop a method to estimate the dose in the patient's body based on the measured calibration units (CU) values.

Material and methods. The material consists of 53 patients treated for prostate cancer with the VMAT technique. The CU signal is measured during the treatment and its value is then transformed according to the self-developed algorithm into a dose. This delivered dose is then compared with the planned dose in the target.

Results. The performed measurements of the CU and preliminary calculations indicate that it is possible to estimate the dose that the patient receives during the therapeutic session. The mean difference between the prescribed and measured dose values is less than 1%, however, there are differences of 17%.

Conclusions. The proposed method can be used in clinical practice for actual dose estimation. The uncertainty of the proposed method was estimated at 5%. In the event of differences above 10%, the treatment realization should be verified by additional tests including patient positioning and technical tests of accelerator, such as verification of kV and MV isocenter compatibility.

Key words: EPID, verification, CU values, *in vivo*

Introduction

An important milestone in improving the quality of radiotherapy worldwide was the development of the multi-leaf collimator (MLC). The original intention of the MLC was to define the shape of the therapeutic beam only, but it significantly increased the protection of critical organs. The full use of all the possibilities of MLC was possible thanks to the concept of inverse planning proposed by Thomas Bortfeld (at the turn of the 20th and the 21st centuries), which led to the implementation of dynamic radiotherapy techniques (IMRT, VMAT). Dynamic techniques were introduced primarily to increase the protection of critical organs, but their capabilities also allowed for the generation of intentional inhomogeneities in the irradiated area (in particular in the target) [1–9].

Jak cytować / How to cite:

Ślosarek K, Gądek A, Reudelsdorf-Ullmann M, Sroka Ł, Winiecki J,. ***The prototype of EPID-based*** **in vivo** ***dose verification for VMAT treatments in patients with prostate cancer.*** *NOWOTWORY J Oncol* 2023; 73: 10–17.

Contemporary techniques used in radiotherapy are characterized by a very high conformality. This means that the dose is delivered very precisely, using steep dose gradients between the target area and the surrounding tissues. Any abnormality (e.g., incorrect patient positioning or changing anatomical conditions as a result of bladder filling) may result in incorrect irradiation. Therefore, it is essential to use the IGRT technique [10–12]. Accurate positioning of the patient and precise reconstruction of the therapeutic position in each fraction is a necessary condition for treatment. The verification of the positioning is mainly carried out on the basis of kV imaging, before or after irradiation (sometimes also during a therapeutic session). Imaging methods allow for checking the geometry of the irradiation. The methods make it possible to increase the local tumor control probability (TCP). Each geographical error will reduce the TCP and increase the probability of complications [13].

Unfortunately, the success of radiotherapy depends not only on the precise positioning of the patient. Another issue is the compliance of the delivered dose with the planned one [14–18]. Before the era of dynamic techniques, *in vivo* dosimetry was widely used in radiotherapy for dose monitoring [19–21]. Dynamic techniques have made this method of dose verification very difficult to use as the dose at the measuring point changes dynamically. The typical dosimeters used, i.e., thermoluminescent ones, unfortunately cannot cope with measurements in which the beam intensity changes and the dose differs at the neighboring points. The known methods of *in vivo* measurement were burdened with very high measurement uncertainty. Modulation of dose distribution made it necessary to verify the dose for the entire irradiated plane, not only in the beam central axis (CAX). Due to technological reasons, the verification of dynamic techniques is currently carried out without the participation of the patient and is limited to checking whether the therapeutic device implements the treatment plan correctly [22–29].

During more than twenty years of the use of dynamic techniques in radiotherapy, many recommendations for quality control have been developed [30–34]. However, they only consider pre-treatment verification without the patient. It is assumed that if the plan is correctly implemented on the measuring phantom, it will be correctly performed with the patient. Increasingly, an independent system for calculating the dose distribution (number of monitor units) is used instead of the measurement. In many countries, checking the dose distribution before the first fraction is a formal and legal requirement [35, 36].

Recently, there has been a rapid development of systems for detection of the fluence of megavoltage radiation. For example, EPID (electronic portal imaging devices), which have been used in radiotherapy for many years, are used for this purpose [37]. They appeared as additional equipment for accelerators before the appearance of the devices dedicated to imaging and IGRT implementation, known to us today. Over time, they have become an integral part of treatment units. EPID and CBCT systems, as imaging tools, are used to verify the patient's position during a therapeutic session and to assess the repeatability of treatment in subsequent fractions [38-44]. Many years ago, attempts were made to correlate the signal read by EPID expressed in so-called calibration units (CU) with the dose during the therapy session [45]. Currently, the literature on the use of this device (EPID) for dose estimation and distribution is very extensive [46–52]. Numerous attempts have been made to calculate the dose in a patient (in space) from the measurement of the signal in a plane, in matrix of semiconductor detectors [46, 53, 54]. The proposed algorithms are usually very complicated and have unit-related limitations (e.g. they relate to a specific therapeutic accelerator) that make their application difficult. They are used only in radiotherapeutic centers that have great scientific and experimental potential. Therefore, the question arises whether they have matrix semiconductor detectors integrated with the accelerator (EPID), it is possible to estimate the dose at the point, placed in the patient.

Aim

The aim of this study was to create a method of estimating the dose at the target area (tumor) received by a patient during a therapeutic session in the VMAT technique. The parameter, which is measured directly, is the signal recorded by the EPID matrix directly behind the patient (acquired image). This method of dose measurement is often called transit dosimetry. On its basis, withreference to the data obtained in the phantom experiment, the average dose received by the patient in the tumor area will be estimated. A low level of complexity of the method is assumed in order to enable its popularization in other radiotherapeutic centers. The parameter describing the quality of the procedure will be the deviation of the estimated dose delivered to the patient (from EPID), compared to the expected value read from the treatment planning system (TPS). As the measurement is performed in real time, it can be considered an *in vivo* method.

Material and methods

The experiment was carried out on Edge, a C-Arm biomedical accelerator (varian medical system, Palo Alto, US) equipped with an aS 1200 EPID detector. We limited the study to 6 MV FFF therapeutic beams only. The control group consisted of patients with diagnosed prostate cancer who underwent radiotherapy at the Radiation Therapy Department of Maria Sklodowska-Curie National Research Institute of Oncology, Gliwice Branch, in Poland. Radiotherapy planning was performed using TPS Eclipse v.16.1 (varian medical systems, Palo Alto, USA).

The measurement system was calibrated using the TMR method. The purpose of the procedure was to correlate the CU value read by the EPID with the actual absorbed dose deposi-

ted in the patient's body at the isocentric point. The influence the distance of the matrix from the phantom bottom-surface (DEP) and the dose deposited in the isocenter (D_{iso}) have on the value of the signal recorded by the EPID was checked.

During the experiment the EPID (detector) was positioned at a constant distance of 160 cm from the source (source imager distance – SID). It should be noted here that the dose estimation at the isocenter is performed only for the VMAT technique with full gantry rotation around the patient (phantom). Due to the rotation of the gantry, the distance DEP fluctuates as a function of the arm position and depends on the dimensions of the patient (phantom).

First, the linearity of the EPID response (CU reading) was checked against the dose deposited in the isocenter. The check was done using a phantom made of PMMA plates with dimensions of 30 x 30 cm^2 and a thickness of 1 cm, which formed a cuboid with the dimensions 30 x 20 x 20 cm^3. The dose prescription point was always located in the center of the phantom, at the isocenter, at a depth of 10 cm (SSD = 90 cm). Measurements were performed for a 6 MV-FFF beam with dimensions of 10 x 10 cm^2, with a 0° gantry position. The CU readings were performed at the SID = 160 cm position, i.e., at a distance of 50 cm below the lower surface of the phantom (the influence of the therapeutic table was considered negligible). The dose value at the isocenter varied from 0.5 Gy to 5.0 Gy.

In the next stage, it was checked what influence DEP distance has on the value of the signal recorded by EPID. The dose at the bottom surface of the phantom D_{out} can be calculated as a function of D_{iso} and the phantom thickness AP using the TMR function. We treat the point on the lower surface of the phantom where D_{out} is defined as the source of the radiation recorded by the EPID.

It is obvious that for different phantom thicknesses there is a relationship: if $AP_1 > AP_2$ then $DEP_2 > DEP_1$. With a fixed D_{out} value, CU_1 will be greater than CU_2. This is in line with the principle that an increase in the distance between the radiation source and the detector reduces the intensity of the recorded radiation. Figure 1 shows the assumptions of this measurement.

It should be noted that the accelerator arm rotates during the procedure, which means that the DEP in the case of a real patient, as well as the depth of the isocentric point are not constant in time (fig. 2).

The dependence of CU on the DEP distance was investigated using the possibility of adjusting the thickness of the plate phantom (AP). The AP thickness was varied in the range of 6–30 cm, which gives the DEP a variation range of 45–57 cm. Using the TMR function, the dose D_{iso} was prescribed in such a way as to maintain a constant D_{out} value for each set of AP and DEP distances.

It should be noted that in the phantom experiment the depth of the dose prescription d (d = 0.5 AP) is similar to the equivalent path length d_{EPL} [55], as the density of the phantom material is similar to the density of water. The physical depth d (or d_{avg}) is needed to determine DEP and d_{EPL} to calculate D_{out} for a known D_{iso}. In the case of the PMMA phantom, these two values are equal. However, in the case of a real patient, the radiological depth differs from the geometric depth due to the non-uniform density. In calculations for

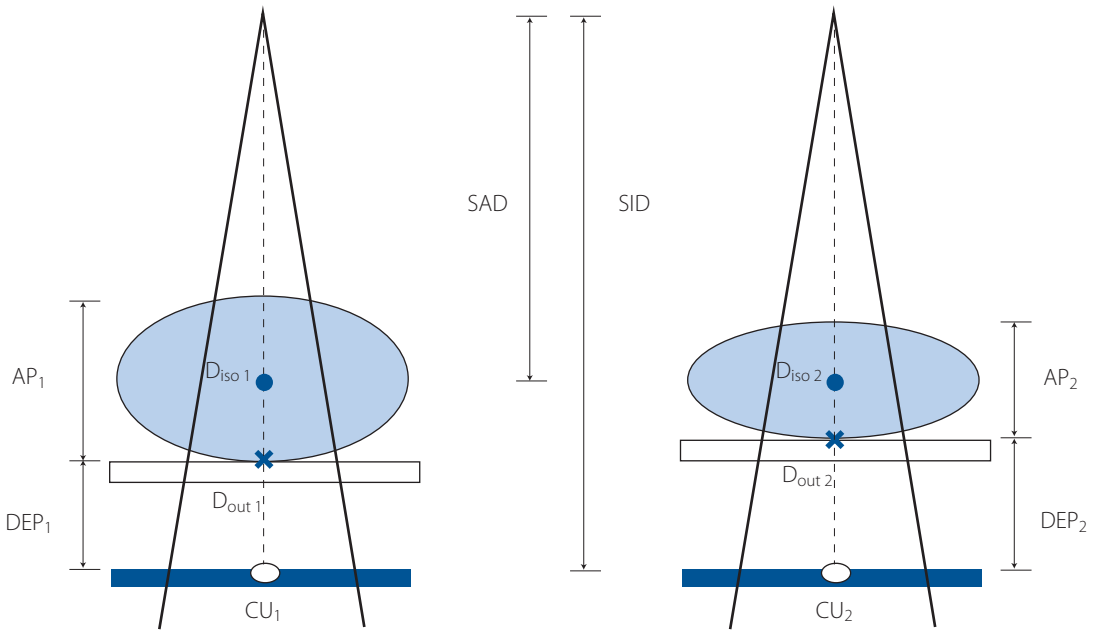

Figure 1. The method of investigating the relationship between the CU value and the D_{out} for different patient thicknesses (phantom dimensions). Explanation of symbols in the text

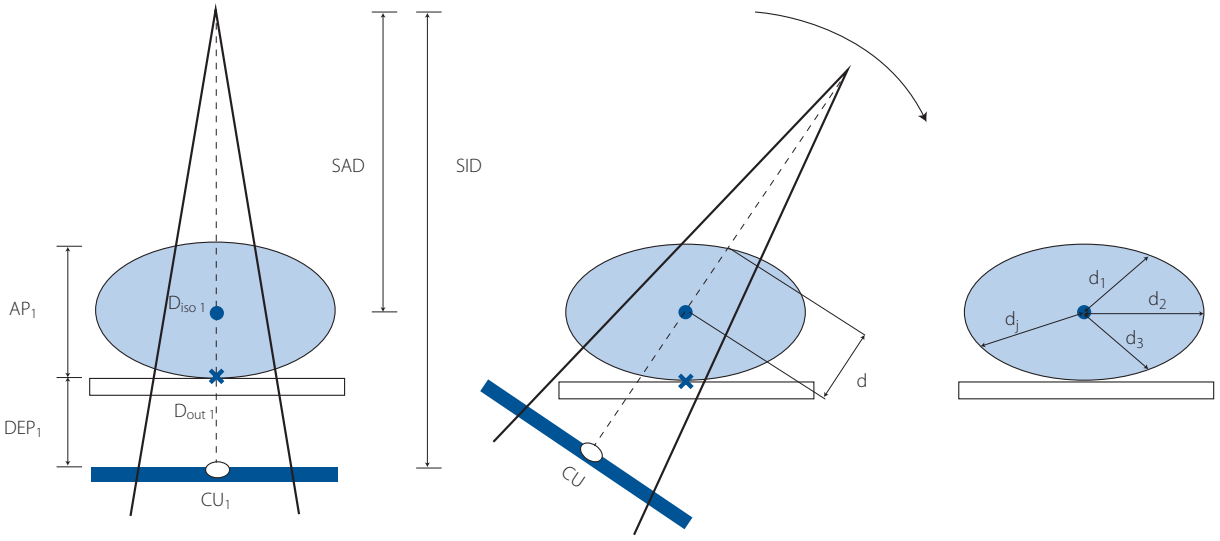

Figure 2. The method of D_{iso} determination: SAD – source axis distance, defines the position of the isocenter, the point at which the dose was prescribed; d_1, d_2, d_3, and d_4 – depths of isocenter for selected angles (gantry positions). The dose at the isocenter (D_{iso}) is dependent on the average depth (d_{avg})

actual patients at full gantry rotation, the mean geometric depth d_{avg} and the mean $d_{EPL,\,avg}$ should be used. The values of d_{avg}, $d_{EPL,avg}$ and D_{iso} can be read from the treatment plan. D_{out} can be derived knowing the DEP and the CU value read from the EPID matrix. It was assumed that this correlation can be derived as follows:

$$D_{out} \sim CU \tag{1}$$

$$D_{out} \sim \frac{1}{DEP^2} \tag{2}$$

$$D_{out} \sim \frac{W1 \times CU}{W2 \times DEP^2 + W3} - W4 \tag{3}$$

Formula (3) is an empirical formula resulting from the reflections of researchers. So we get:

$$CU = \frac{(D_{out} + W4) \times (W2 \times DEP^2 + W3)}{W1} \tag{4}$$

Formula (4) will be used to calculate the coefficients W1, W2, W3, and W4 in phantom measurements. The values will then be used to calculate D_{iso} in the patient during transit dosimetry.

In the case with a real patient, the EPID detector records the CU value during a therapeutic session. Thus, the D_{out} at surface in the first step and then the D_{iso} within the body can be calculated using the mean depth value and the TMR value.

To calculate the dose at the isocenter point in the patient (D_{iso}^{EPID}), the following formula is used:

$$D_{iso}^{EPID} = D_{out} \times \frac{TMR(2d_{EPL})}{TMR(d_{EPL})} \tag{5}$$

and considering that DEF = SID–SAD + d_{avg} = 60 + d_{avg}, we get:

$$D_{iso}^{EPID} = \frac{W1 \times CU + W3}{TMR(d_{EPL})} \times \frac{TMR(2d_{EPL})}{TMR(d_{EPL})} \tag{6}$$

where:

- CU – mean value of the signal registered in the central part of the EPID matrix, a set of points located at a distance of no more than 1 cm from CAX,
- d_{avg} [cm] – average depth of the dose prescription point (isocenter), value determined from the treatment planning system resulting from the rotation of the head around the patient,
- SID – source imager distance (consider fig. 1 and fig.2).

The deviation between the D_{iso}^{EPID} dose value (calculated from the CU measured during the therapeutic session) and the D^{TPS}_{iso} dose in the isocenter (calculated in the treatment planning system) was calculated using the formula:

$$\%\Delta = \frac{D_{iso}^{EPID} - D_{iso}^{TPS}}{D_{iso}^{TPS}} \times 100\% \tag{7}$$

In order to verify the correctness of the model, calculations of the dose distribution were performed for a cuboid-shaped polystyrene phantom in the TPS system. The phantom was then irradiated by setting the calculated number of MU_{PMMA}. EPID recorded radiation passing through the phantom CU_{PMMA}. The PMMA phantom was then changed to a CIRS Thorax (lungs) and the exposure was repeated with the same settings (including MU_{PMMA}). This time CU_{CIRS} was registered. For both cases (CU_{PMMA} and CU_{CIRS}) the D_{iso}^{EPID} was determined. Two phantoms with different density homogeneity were used. The PMMA phantom has uniform densities throughout the volume. The CIRS phantom has a very heterogeneous density in the tested volume (lung tissue, bone, soft tissue). If dose was calculated for of PMMA phantom but irradiated was phantom CIRS (slightly different in density) the difference in the measured EPID signal should be "pronounced". And the described method is to ensure, above all, the detection of a significant error.

The clinical material consists of 53 patients treated for prostate cancer. The VMAT technique (full rotation) was used, a fractionation of 5 fractions at 7.25 Gy (isodose 98%) per fraction, up to a total dose of 36.25 Gy. Dose distribution calculations were performed using Eclipse treatment planning system (Varian Medical Systems) with the Acuros v.16.1 algorithm. Imaging examinations dedicated to treatment planning were performed on a Somatom go.Open Pro-/S or Somatom Definition AS CT-scanners from Siemens AG Germany. The treatment was carried out on the Edge v.2.7 accelerator (Varian Medical System), equipped with the EPID aS 1200 detector. 6 MV-FFF beams were used for all patients.

Results

Phantom measurements

Figure 3 shows the relationship between the dose (D_{out}) and the CU value for different DEP values (40, 50, and 60 cm). In the dose range: 0.24 Gy it is a linear relationship, the R^2 coefficient is equal to unity. Thus, we consider the measured CU signal to be directly proportional to the radiation dose.

Table I shows the correlation between CU and dose D_{out}. For selected clinical situations (differing in the D_{out} and DEF values), the CU measurement was performed and then compared with a value calculated in accordance with formula 4.

Analyzing table I, it can be seen that the dispersion of differences %Δ between the calculated and measured CU value ranges from –1.92% to 3.17%. Therefore, the uncertainty of this method can be assumed to be ≈5% (3.17 – (–1.92) = 5.09). The Wilcoxon test for these sets showed no statistically significant differences ($p > 0.05$).

Validation

As part of the method validation, the treatment plan was prepared for PMMA homogeneous phantom, which was then irradiated. We recorded the output signal with EPID and then the PMMA phantom was replaced with the CIRS Thorax phantom. It was then irradiated with the same beam parameters as a homogeneous phantom.

The reconstructed D_{iso}^{EPID} dose value for the PMMA phantom differed from the ordered D_{iso} by –5.39%, while the replacement of the phantom with the CIRS caused a significant difference of 164.44% (!) of the expected value.

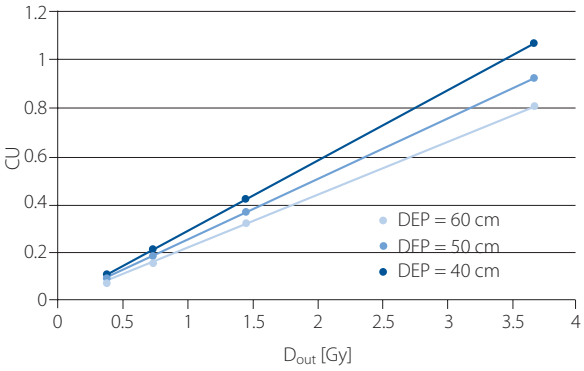

Figure 3. Dependence of the CU value on the dose (D_{out}) and the DEP value, for the 6 MV-FFF beam, with a size of 10 x 10 cm, SID = 160 cm

Table I. Deviation of the calculated CU value from the measured value for selected clinical situations

DPE (cm)	D_{out} (Gy)	CU measured	CU calculated	%Δ
60	0.367	0.080	0.080	0.10%
60	0.734	0.161	0.160	–0.47%
60	1.451	0.322	0.316	–1.92%
60	3.670	0.806	0.798	–0.93%
50	0.367	0.092	0.095	3.17%
50	0.734	0.184	0.190	2.85%
50	1.451	0.369	0.374	1.18%
50	3.670	0.924	0.944	2.10%
40	0.367	0.107	0.107	0.09%
40	0.734	0.214	0.213	–0.35%
40	1.451	0.428	0.421	–1.81%
40	3.670	1.072	1.063	–0.85%

Measurements with the patient

For each patient, the CU measurements were performed using the EPID device during all fractions. The detector was always set at SID = 160 cm. The basic parameters of the treatment plan for the patients are presented in table II.

The average number of arcs is 3. The minimum number of MUs for a plan is 1803 MU and the maximum is 4232 MU, which gives an average value of 2966 MU.

The mean difference between the planned dose (D_{iso}^{TPS}) and the measured one (D_{iso}^{EPID}) for the 53 patients analyzed is

Table II. Basic parameters describing treatment plans included in the experiment

	Number of arcs	sum of MU's	d_{avg} [cm]	$d_{EPI, avg}$ [cm]
average	3	2966	17.3	15.9
max	4	4232	19.6	18.0
min	2	1803	14.6	13.3

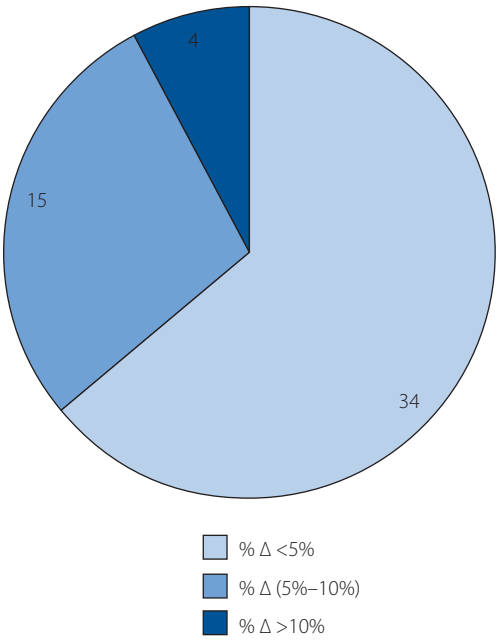

Figure 4. The number of cases for the deviation between the planned and measured dose using the proposed method based on EPID measurements. For over 60% of cases, the difference was less than 5%

less than 1%, the maximum noticed difference is 17%. In 64% of the analyzed cases, the difference between the planned and measured dose was lower by 5%. In 28% of cases, the difference ranged from 5–10%, in the remaining 7% (four patients) it exceeded 10% (fig. 4).

Since in a few cases the difference %Δ exceeded 10%, the relationship between the complexity of the plan and the investigated parameter %Δ was analyzed. Plan complexity was defined as the number of monitor units per arc. No such correlation has been found.

The mean difference between the planned dose and the measured dose is 0.9%. However, the maximum values of the differences were 17%. Statistical tests (Wilcoxon) did not show a statistical significance between the set of doses in the ISO, both the planned and measured one.

Discussion

The proposed method of dose verification does not require any additional procedures. It does not extend the time of the patient's preparation for the therapeutic session and the total time spent in the therapeutic room. The method allows to estimate the actual dose that the prostate cancer patient receives during the VMAT therapy. We denote the uncertainty of the method as 5%. Reducing this uncertainty in the future can be achieved by introducing into the formulas dependencies on the dimensions of the fields, which change significantly in dynamic techniques. Undoubtedly, the lack of this value in the calculation method affects the results. Discrepancies may occur when the dose prescription point does not coincide with the beam CAX. As described, the CU is read from the center of the matrix through which the CAX passes. We suspect that the method may be less accurate if the dose prescription point is in the area of significant heterogeneities, where small absolute differences between calculated dose and the measured one translate into relatively large percentage differences.

The phantom experiment has shown that using the wrong treatment plan or irradiating the wrong patient will result in differences that far exceed the uncertainty of the method. Such large differences, in this case, are explained by significant differences in the geometry of the phantoms and their density.

However, for over fifty patients, the sets of planned and measured doses do not show a statistically significant difference. The average error is around 1%.

In 4 out of 53 cases, the differences in planned and measured doses were greater than 10%. This happened despite the fact that each patient had IGRT applied, so it is necessary to assume the correct reconstruction of the therapeutic position (geometry). As already mentioned, we found no correlation between the number of MUs per arc and the %Δ. However, it is true that with a %Δ greater than 10%, the number of MUs per arc was as much as 20% higher than where %Δ was less than 5%. Therefore, although this has not been clarified, it is worth considering the complexity of the treatment plan when assessing the differences between calculated and measured doses.

Of course, this method can be considered complementary to the verification process, but in its current form it cannot be considered as an *in vivo* method in the VMAT technique. However, combining it with the treatment repeatability assessment presented in [39], it can be successfully used to verify the dose delivered during a therapeutic session.

Conclusions

The developed method of comparing the dose in a patient measured by EPID and the planned one can be used in clinical practice to estimate the dose that a patient receives during therapeutic sessions. The uncertainty of the method is at the level of 5%. Unfortunately, there are situations where the differences between the planned and measured dose are greater than 10%. In this case, the first step is to assess the complexity of the treatment plan (e.g. the number of monitor units per arc).

Conflict of interest: none declared

Adam Gądek
Maria Sklodowska-Curie National Research Institute of Oncology
Gliwice Branch
Radiotherapy Planning Department
Wybrzeże Armii Krajowej 15
44-102 Gliwice, Poland
e-mail: adam.gadek@io.gliwice.pl

Received: 30 Oct 2022
Accepted: 20 Jan 2023

References

1. Slosarek K, Rembielak A, Cramb J, et al. Pitfalls in IMRT treatment planning with the CadPlan-Helios system. Med Dosim. 2004; 29(3): 179–183, doi: 10.1016/j.meddos.2004.04.005, indexed in Pubmed: 15324914.
2. Ślosarek K, Składowski K, Rembielak A, et al. Intensity modulated Radiation Therapy (IMRT) - description of the irradiation technique. Nowotwory. 2001; 51(6): 614–618.
3. Składowski K, Grządziel M, Hutnik M, et al. Clinical principles of planning and implementation IMRT techniques in patients with head and neck cancer - part 1. Onkol Prakt Klin Edu. 2007; 3(5): 241–248.
4. Ślosarek K, Bekman B, Wendykier J, et al. In silico assessment of the dosimetric quality of the novel, automated radiation treatment planning strategy for linac-based radiosurgery of multiple brain metastases and a comparison with robotic methods. Radiation Oncology. 2018; 13(1).
5. Slosarek K, Zajusz A, Szlag M. Comparison of traditional and simultaneous IMRT boost technique basing on therapeutic gain calculation. Med Dosim. 2008; 33(4): 299–302, doi: 10.1016/j.meddos.2008.02.001, indexed in Pubmed: 18973858.
6. Ślosarek K. Techniki dynamiczne generujące zróżnicowany rozkład dawki promieniowania w radioterapii. Reports of Practical Oncology & Radiotherapy. 2003; 8: 9–83, doi: 10.1016/s1507-1367(01)70484-1.
7. Oelfke U, Bortfeld T. Inverse planning for x-ray rotation therapy: a general solution of the inverse problem. Phys Med Biol. 1999; 44(4): 1089–1104, doi: 10.1088/0031-9155/44/4/019.
8. Oelfke U, Bortfeld T. Intensity modulated radiotherapy with charged particle beams: Studies of inverse treatment planning for rotation therapy. Med Phys. 2000; 27(6): 1246–1257, doi: 10.1118/1.599002.
9. Oelfke U, Bortfeld T. Inverse planning for photon and proton beams. Medical Dosimetry. 2001; 26(2): 113–124, doi: 10.1016/s0958-3947(01)00057-7.
10. Grills IS, Hugo G, Kestin LL, et al. Image-guided radiotherapy via daily online cone-beam CT substantially reduces margin requirements for stereotactic lung radiotherapy. Int J Radiat Oncol Biol Phys. 2008; 70(4): 1045–1056, doi: 10.1016/j.ijrobp.2007.07.2352, indexed in Pubmed: 18029110.
11. van Elmpt W, Nijsten S, Petit S, et al. 3D in vivo dosimetry using megavoltage cone-beam CT and EPID dosimetry. Int J Radiat Oncol Biol Phys. 2009; 73(5): 1580–1587, doi: 10.1016/j.ijrobp.2008.11.051, indexed in Pubmed: 19306755.
12. van Elmpt W, Petit S, De Ruysscher D, et al. 3D dose delivery verification using repeated cone-beam imaging and EPID dosimetry for stereotactic body radiotherapy of non-small cell lung cancer. Radiother Oncol. 2010; 94(2).
13. Maciejewski B, Drzewiecka B, Ślosarek K, et al. Physical and radiobiological rationale for advantages and limitations for Intensity-Modulated Radiotherapy (IMRT). Nowotwory. 2001; 51(4): 355–364.
14. Olaciregui-Ruiz I, Rozendaal R, van Kranen S, et al. The effect of the choice of patient model on the performance of in vivo 3D EPID dosimetry to detect variations in patient position and anatomy. Med Phys. 2020; 47(1): 171–180, doi: 10.1002/mp.13893, indexed in Pubmed: 31674038.
15. McDermont LN, Wedling M, Sonke JJ, et al. Replacing pretreatment verification with in vivo EPID dosimetry for prostate IMRT. Int J Radiation Oncology Biol Phys. 2007; 67(5): 1568–1577.
16. McDermott LN, Wendling M, Nijkamp J, et al. 3D in vivo dose verification of entire hypo-fractionated IMRT treatments using an EPID and cone-beam CT. Radiother Oncol. 2008; 86(1): 35–42, doi: 10.1016/j.radonc.2007.11.010, indexed in Pubmed: 18061692.
17. van Zijtveld M, Dirkx MLP, de Boer HCJ, et al. 3D dose reconstruction for clinical evaluation of IMRT pretreatment verification with an EPID. Radiother Oncol. 2007; 82(2): 201–207, doi: 10.1016/j.radonc.2006.12.010, indexed in Pubmed: 17287039.
18. Li Y, Zhu J, Shi J, et al. Investigating the effectiveness of monitoring relevant variations during IMRT and VMAT treatments by EPID-based 3D in vivo verification performed using planning CTs. Comparative Study. 2019; 14(6).
19. van Dam GMJ. Methods for in vivo dosimetry in external radiotherapy. ESTRO, Brussels 1994.
20. IAEA. Development of Procedures for In Vivo Dosimetry in Radiotherapy. IAEA, Vienna 2013.
21. Mijnheer B, Beddar S, Izewska J, et al. *In vivo* dosimetry in external beam radiotherapy. Med Phys. 2013; 40(7): 070903, doi: 10.1118/1.4811216.
22. Sekaran S, Arjunan M, Sarkar B, et al. Electronic portal imaging device--based three-dimensional volumetric dosimetry for intensity-modulated radiotherapy pretreatment quality assurance. J Med Phys. 2019; 44(3): 176, doi: 10.4103/jmp.jmp_42_19.
23. McDermott L. On radiotherapy dose verification with a flat-panel imager. Radiother Oncol. 2009; 92(1).
24. Alber M, Broggi S, De Wagter C, et al. GUIDELINES FOR THE VERIFICATION OF IMRT. 2008.
25. Alber M, Broggi S, De Wagter C, et al. Guidelines for the verification of IMRT. ESTRO, Brussels 2008.
26. Zhang J, Li X, Lu M, et al. A method for in vivo treatment verification of IMRT and VMAT based on electronic portal imaging device. Radiation Oncology. 2021; 16(232).
27. Winiecki J, Morgaś T, Majewska K, et al. The gamma evaluation method as a routine QA procedure of IMRT. Rep Pract Oncol Radiother. 2009; 14(5): 162–168, doi: 10.1016/S1507-1367(10)60031-4.
28. Winiecki J, Żurawski Z, Drzewiecka B, et al. Anatomy-corresponding method of IMRT verification . Rep Pract Oncol Radiother. 2011; 16(1): 1–9, doi: 10.1016/j.rpor.2010.11.001 .
29. Klimas A, Grządziel A, Plaza D, et al. EPID – a useful interfraction QC tool. Polish Journal of Medical Physics and Engineering. 2019; 25(4): 221–228, doi: 10.2478/pjmpe-2019-0029.
30. Ślosarek K. Verification of realization dynamic techniques in radiotherapy. Inżynier i Fizyk Medyczny. 2013; 2: 243–252.
31. Miften M, Olch A, Mihailidis D, et al. Tolerance limits and methodologies for IMRT measurement-based verification QA: Recommendations of AAPM Task Group No. 218. Med Phys. 2018; 45(4): e53–e83, doi: 10.1002/mp.12810, indexed in Pubmed: 29443390.
32. van Zijtveld M, Dirkx MLP, de Boer HCJ, et al. Dosimetric pre-treatment verification of IMRT using an EPID; clinical experience. Radiother Oncol. 2006; 81(2): 168–175, doi: 10.1016/j.radonc.2006.09.008, indexed in Pubmed: 17055604.
33. Herman M, Balter J, Jaffray D, et al. Clinical use of electronic portal imaging: Report of AAPM Radiation Therapy Committee Task Group 58. Medical Physics. 2001; 28(5): 712–737, doi: 10.1118/1.1368128.
34. Kupelian PA, Lee C, Langen KM, et al. Evaluation of image-guidance strategies in the treatment of localized prostate cancer. Int J Radiat Oncol Biol Phys. 2008; 70(4): 1151–1157, doi: 10.1016/j.ijrobp.2007.07.2371, indexed in Pubmed: 17892920.
35. Ustawa Prawo Atomowe - Dziennik Ustaw 2021, poz.623.
36. Obwieszczenie Ministra Zdrowia z dnia 3 kwietnia 2017 w sprawie warunków bezpiecznego stosowania promieniowania jonizującego dla wszystkich rodzajów ekspozycji medycznej 2017.
37. Grządziel A, Smolińska B, Rutkowski R, et al. EPID dosimetry – configuration and pre-treatment IMRT verification. Reports of Practical Oncology & Radiotherapy. 2007; 12(6): 307–312, doi: 10.1016/s1507-1367(10)60069-7.
38. van Elmpt W, McDermott L, Nijsten S, et al. A literature review of electronic portal imaging for radiotherapy dosimetry. Radiother Oncol. 2008; 88(3): 289–309, doi: 10.1016/j.radonc.2008.07.008, indexed in Pubmed: 18706727.
39. Mans A, Wendling M, McDermott LN, et al. Catching errors with*in vivo*EPID dosimetry. Med Phys. 2010; 37(6Part2): 2638–2644, doi: 10.1118/1.3397807.
40. Gabryś D, Kulik R, Trela K, et al. Dosimetric comparison of liver tumour radiotherapy in all respiratory phases and in one phase using 4DCT. Radiother Oncol. 2011; 100(3): 360–364, doi: 10.1016/j.radonc.2011.09.006, indexed in Pubmed: 21974916.
41. Woźniak G, Dolla Ł, Ślosarek K, et al. Dynamic-arc respiratory-gated stereotactic radiotherapy — technique presentation. Nowotwory. Journal of Oncology. 2018; 67(5): 297–300, doi: 10.5603/njo.2017.0049.
42. Ślosarek K, Plaza D, Nas A, et al. Portal dosimetry in radiotherapy repeatability evaluation. J Appl Clin Med Phys. 2022; 22(1): 156–164.
43. Baran M, Tabor Z, Kabat D, et al. Isodoses—a set theory-based patient--specific QA measure to compare planned and delivered isodose distributions in photon radiotherapy. Strahlenther Onkol. 2021.

44. Kang S, Li J, Ma J, et al. Evaluation of interfraction setup variations for postmastectomy radiation therapy using EPID-based in vivo dosimetry. J Appl Clin Med Phys. 2019; 20(10): 43–52, doi: 10.1002/acm2.12712, indexed in Pubmed: 31541537.
45. Esposito M, Bruschi A, Bastiani P, et al. Characterization of EPID software for VMAT transit dosimetry. Australas Phys Eng Sci Med. 2018; 41(4): 1021–1027, doi: 10.1007/s13246-018-0693-0, indexed in Pubmed: 30341673.
46. Boutry C, Sors A, Fontaine J, et al. Technical Note: A simple algorithm to convert EPID gray values into absorbed dose to water without prior knowledge. Med Phys. 2017; 44(12): 6647–6653, doi: 10.1002/mp.12587, indexed in Pubmed: 28921931.
47. Moustakis C, Ebrahimi Tazehmahalleh F, Elsayad K, et al. A novel approach to SBRT patient quality assurance using EPID-based real-time transit dosimetry : A step to QA with in vivo EPID dosimetry. Strahlenther Onkol. 2020; 196(2): 182–192, doi: 10.1007/s00066-019-01549-z, indexed in Pubmed: 31925465.
48. Slosarek K, Szlag M, Bekman B, et al. EPID in vivo dosimetry in RapidArc technique. Rep Pract Oncol Radiother. 2010; 15(1): 8–14, doi: 10.1016/j.rpor.2010.01.003, indexed in Pubmed: 24376916.
49. Wendling M, Louwe R, McDermott L, et al. Accurate two-dimensional IMRT verification using a back-projection EPID dosimetry method. Med Phys. 2006; 33(2): 259–273, doi: 10.1118/1.2147744.
50. Rose M, Tirpak L, Casteren KV, et al. Multi-institution validation of a new high spatial resolution diode array for SRS and SBRT plan pretreatment quality assurance. Med Phys. 2020; 47(7): 3153–3164, doi: 10.1002/mp.14153.
51. Kruszyna-Mochalska M. EPID-based daily verification of reproducibility of patients' irradiation with IMRT plans. Rep Pract Oncol Radiother. 2018; 23(5): 309–314, doi: 10.1016/j.rpor.2018.05.003, indexed in Pubmed: 30108458.
52. Mijnheer B, Olaciregui-Ruiz I, Rozendaal R. 3D EPID-based in vivo dosimetry for IMRT and VMAT. Journal of Physics: Conference Series. 2013.
53. Olaciregui-Ruiz I, Vivas-Maiques B, Kaas J, et al. Transit and non-transit 3D EPID dosimetry versus detector arrays for patient specific QA. J Appl Clin Med Phys. 2019; 20(6): 79–90, doi: 10.1002/acm2.12610.
54. Osewski W, Dolla L, Radwan M, et al. Clinical examples of 3D dose distribution reconstruction, based on the actual MLC leaves movement, for dynamic treatment techniques. Rep Pract Oncol Radiother. 2014; 19(6): 420–427, doi: 10.1016/j.rpor.2014.04.013, indexed in Pubmed: 25337416.
55. Kalet I, Kennedy D. A comparison of two radiological path length algorithms. International Journal of Radiation Oncology*Biology*Physics. 1987; 13(12): 1957–1959, doi: 10.1016/0360-3016(87)90366-x.